INT. J. NUM. METH. HEAT FLUID FLOW, VOL. 3, 91–105 (1993)

NATURAL CONVECTION HEAT TRANSFER IN INCLINED TALL CAVITIES BOUNDED BY POROUS LAYERS

M. HASNAOUI, P. VASSEUR AND E. BILGEN

Department of Mechanical Engineering, Ecole Polytechnique, CP 6079, St 'A', Montréal, PQ, H3C 3A7, Canada

ABSTRACT

Thermally driven flow in a tall inclined cavity bounded by porous layers is studied analytically and numerically. A constant heat flux is applied for heating and cooling of two opposing walls of the cavity, while the other two are insulated. The Beavers–Joseph slip condition on velocity is applied at the interface between the fluid and porous layers. An analytical solution is obtained by assuming parallel flow in the core region of the cavity and a numerical solution by solving the complete governing equations. The flow and heat transfer variables are obtained in terms of the Rayleigh number, Ra, slip condition parameter N and angle of inclination of the cavity Φ. The critical Rayleigh numbers for the onset of convection in a layer heated from below are predicted for various hydrodynamic boundary conditions. The results for a fluid layer bounded by solid walls ($N \to \infty$) and by free surfaces ($N \to 0$) emerge from the present analysis as limiting cases.

KEY WORDS Beavers–Joseph slip condition Natural convection flow Critical Rayleigh numbers

NOMENCLATURE

A	aspect ratio, H'/L'	Pr	Prandtl number, ν/α
C	dimensionless temperature gradient along y direction	q'	constant heat flux
		Ra	Rayleigh number, $(g\beta q' L'^4)/(k\nu\alpha)$
g	acceleration due to gravity		
H'	length of the system	Ra_C	critical Rayleigh number
k	thermal conductivity of the fluid	S	surface tension gradient with respect to temperature
K	permeability of the porous medium	T	dimensionless temperature, $(T' - T'_0)/(q'L'/k)$
L'	thickness of the system		
Ma	Marangoni number, $q'SL'^2/(k\alpha\mu)$	T'_0	reference temperature at $x' = y' = 0$
Ma_C	critical Marangoni number	ΔT	dimensionless temperature difference at $y = 0$, $(T_{(1/2,0)} - T_{(-1/2,0)})$
N, N_1, N_2	slip coefficient parameters in the Beavers–Joseph condition		
Nu	mean Nusselt number	u, v	dimensionless velocities in x and y directions, $(u', v')L'/\alpha$
p	dimensionless pressure, $(p' + \rho g y' \sin\Phi - \rho g x' \cos\Phi)/\rho(\alpha/L')^2$	x, y	dimensionless Cartesian coordinates, $(x', y')/L'$

0961-5539/93/020091-15$2.00

Received January 1992
Revised October 1992

Greek symbols

α	thermal diffusivity of fluid medium
$\bar{\alpha}, \bar{\alpha}_1, \bar{\alpha}_2$	constants of proportionality in the Beavers–Joseph condition, $\bar{\alpha}L'/K^{1/2}$
β	coefficient of thermal expansion of fluid
ω	dimensionless vorticity
θ	dimensionless temperature
ν	kinematic viscosity
ρ	fluid density
σ	surface tension
Ψ	dimensionless stream function, Ψ'/α
Φ	angle of cavity inclination

Superscript

	dimensional variables

INTRODUCTION

Natural convection in fluid-filled rectangular cavities has received considerable attention over the past several years, largely due to its direct relevance in a variety of applications. Comprehensive review of this literature has been given recently by Bejan[1]. Most of the previous work has addressed natural convection in a cavity bounded by rigid impervious walls. Rather little work has been carried out for more complex boundary conditions such as the case when the flows are bounded by porous layers. Such a model comes closest to simulating the situation that exists in thermal reactors (nuclear, chemical, thermal), and in the building technology.

The interaction that occurs at the interface between a fluid and a porous layer has been formulated in the past according to two approaches. One is to use the Brinkman equation for the porous layer with the continuity of velocity and shear as interface conditions. Using this approach, Somerton and Catton[2] studied the stability of a system consisting of a volumetrically heated porous bed saturated with and overlaid with a fluid, heated or cooled isothermally from below. The natural convective heat transfer in a rectangular cavity partially filled with a porous medium has been numerically investigated by Arquis and Caltagirone[3]. Using the Brinkman extended model, the porous medium was considered to be a special fluid so that no explicit expression of boundary conditions at the interface was needed. The same problem was considered by Nishimura *et al.*[4] using a Brinkman model. However, the boundary conditions at the interface between fluid and porous media were written explicitly in stream function–vorticity form. Their numerical results were in good agreement with experimental data. More recently, the thermal instability and natural convection heat transfer were studied analytically by Vasseur *et al.*[5] for a porous bed under a fluid in a shallow cavity heated from bottom by a constant heat flux. Closed form solutions were obtained using Navier–Stokes and Brinkman's equations for the fluid motion in fluid and porous regions respectively. The other approach is to employ Darcy's equation for the porous layer with the Beavers–Joseph condition[6] (hereafter called BJ) as one of the interface conditions. Nield[7,8] applied this method to study the onset of convection in a horizontal layer of fluid overlying a porous layer and a porous layer sandwiched between two fluid layers respectively. Exact solutions were obtained for constant-flux thermal boundary conditions. His work was initiated as an approach to incorporate the non-slip condition on rigid boundaries for the Rayleigh–Darcy problem. The same configuration as the one studied by Nield was also considered by Pillatsis *et al.*[9] for more general boundary conditions. The critical Rayleigh number and the horizontal wave number for the onset of convective motion were found to depend, among others, on the proportionality constant in the BJ condition. The BJ condition was also considered by Chen *et al.*[10] in their study of the onset of thermal convection due to heating from below in a system consisting of a fluid layer overlying a porous layer with anisotropic permeability and thermal diffusivity. Buoyancy driven flow in a vertical slot bounded by porous layer was studied recently by Murthy and Rudraiah[11]. Analytical solutions, valid in the boundary layer regime, were obtained using the BJ slip condition on velocity, and uniform

heat flux at the interface. It was found that the effect of the BJ slip condition was to increase the heat transfer.

In the present investigation, the behaviour of natural convection in a tilted fluid cavity bounded by porous layers is studied analytically and numerically. A constant heat flux is applied for heating and cooling the two opposing walls of the cavity while the other two are insulated. A parallel flow approximation is used, which enables the temperature and velocity field in the core region to be determined analytically. A numerical study is also carried out on the same problem.

GOVERNING EQUATIONS AND BOUNDARY CONDITIONS

The physical configuration selected for analysis is shown in *Figure 1*. The two-dimensional inclined cavity, of dimensions $L' \times H'$, is bounded on the long sides by thin porous layers. They are subjected to uniform heat flux q', while the short end walls are impermeable and adiabatic. The thermophysical properties of the fluid at a reference temperature T'_0 are assumed to be constant, except for the density in the buoyancy term in the momentum equation (Boussinesq approximation).

For a two-dimensional steady laminar flow one can write the continuity equation, the Navier–Stokes equations, and the energy equation as follows:

$$\frac{\partial u}{\partial x} + \frac{\partial v}{\partial y} = 0 \tag{1}$$

$$u\frac{\partial u}{\partial x} + v\frac{\partial u}{\partial y} = -RaPrT\cos\Phi - \frac{\partial p}{\partial x} + Pr\nabla^2 u \tag{2}$$

$$u\frac{\partial v}{\partial x} + v\frac{\partial v}{\partial y} = RaPrT\sin\Phi - \frac{\partial p}{\partial y} + Pr\nabla^2 v \tag{3}$$

$$u\frac{\partial T}{\partial x} + v\frac{\partial T}{\partial y} = \nabla^2 T \tag{4}$$

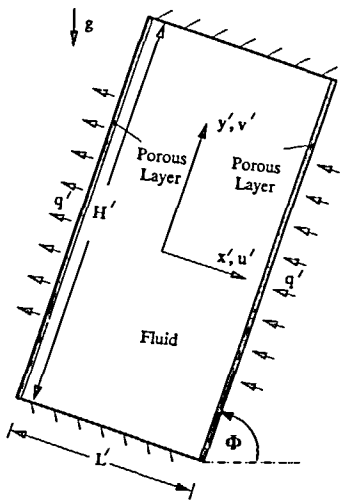

Figure 1 Physical configuration

Equations (1) to (4) have been reduced to dimensionless form by introducing the following scales:

$$\left.\begin{aligned} (x, y) &= (x', y')/L' & (u, v) &= (u', v')/(\alpha/L') \\ p &= (p' + \rho g y' \sin\Phi - \rho g x' \cos\Phi)/(\rho(\alpha/L')^2) & T &= (T' - T_0')/\Delta T' \\ Ra &= \frac{g\beta q' L'^4}{k\alpha\nu} & \Delta T' &= (q'L'/k) \\ Pr &= \nu/\alpha \end{aligned}\right\} \quad (5)$$

The thermal boundary conditions are:

$$y = \pm A/2 \qquad \frac{\partial T}{\partial y} = 0 \quad (6)$$

$$x = \pm 1/2 \qquad \frac{\partial T}{\partial x} = 1 \quad (7)$$

The hydrodynamic boundary conditions are:

$$y = \pm A/2 \qquad u = v = 0 \quad (8)$$

$$x = \pm 1/2 \qquad u = 0; \qquad \frac{\mathrm{d}v}{\mathrm{d}x} = -Nv \quad (9)$$

Equation (8) expresses the no-slip boundary condition on solid boundaries while equation (9) is the BJ condition at the porous–fluid interface. The validity of the BJ condition has been proven both theoretically and experimentally[12–15].

The stream function Ψ is introduced:

$$u = \frac{\partial \Psi}{\partial y} \qquad v = -\frac{\partial \Psi}{\partial x} \quad (10)$$

and the pressure terms in the momentum equations are eliminated by cross-differentiation of (2) and (3), resulting in:

$$J(\Psi, \nabla^2\Psi) = Pr\nabla^4\Psi - RaPr\left[\sin\Phi \frac{\partial T}{\partial x} + \cos\Phi \frac{\partial T}{\partial y}\right] \quad (11)$$

The energy equation (4) can also be expressed as:

$$J(\Psi, T) = -\nabla^2 T \quad (12)$$

where $J(f, g) = f_x g_y - f_y g_x$.

The corresponding boundary conditions for the stream-function will be:

$$y = \pm A/2 \qquad \Psi = \frac{\partial \Psi}{\partial y} = 0 \quad (13)$$

$$x = \pm 1/2 \qquad \frac{\partial^2 \Psi}{\partial x^2} = -N \frac{\partial \Psi}{\partial x} \quad (14)$$

Equations (11) and (12) together with boundary conditions (6)–(9) complete the formulation of the problem. The governing parameters are Ra, Pr, A, Φ and N.

The heat transfer rate across the system can be expressed in terms of a Nusselt number at $y = 0$, defined as:

$$Nu = \frac{1}{\Delta T} \quad (15)$$

The above definition of Nu results from the fact that, as demonstrated in the analytical solution, the temperature of both walls increase linearly with y, at the same rate, so that ΔT is independent of y.

NUMERICAL METHOD

In the numerical solution, the governing equations (1) to (4) were solved using a finite-difference procedure—SIMPLER method[16]. The computer code was validated with the benchmark solution of De Vahl Davis and Jones[17]. The comparison was observed to be very good with a maximum deviation with less than 1.5%.

The hybrid scheme was used and various tests showed that 41×61 grids were generally adequate to correctly describe the flow and heat transfer when the slip conditions are weak ($N \geqslant 50$). However, grids of 61×81 and 81×83 were also used at high Ra numbers and $N \leqslant 20$ to obtain the flow details. A staggered grid was used for velocity to avoid wave pressure and velocity fields. The relaxation parameter was varied from 0.4 for small Ra numbers to 0.05 for large Ra. The convergence criterion was based on the corrected pressure field. When the corrected terms were small enough so that no difference existed between the pressure fields before and after correction, the computation was stopped. Hence,

$$\sum_{i=1}^{imax} \sum_{j=1}^{jmax} |c_{ij}| \leqslant \varepsilon \tag{16}$$

where c_{ij} is the source term in the pressure correction equation (see Patankar[16]) and $\varepsilon \leqslant 0.00005$.

ANALYTICAL SOLUTION

The analytical solution is obtained based on the parallel flow approximation developed by Cormack *et al.*[18] and used by Bejan and Tien[19], Vasseur *et al.*[20,21], Sen *et al.*[22,23] and others. This approximation, valid for narrow cavities ($A \gg 1$), suggests that the velocity and temperature distributions in the central part of the fluid layer, should be of the form:

$$\Psi(x, y) \simeq \Psi(x) \tag{17}$$

$$T(x, y) \simeq Cy + \theta(x) \tag{18}$$

where C is an unknown but constant temperature gradient in the y direction. Because of turning flow at the end regions, the boundary conditions in the y direction cannot be exactly satisfied by the parallel flow approximation. Taking $\Psi = 0$ at $x = \pm 1/2$, however, ensures us that the net flow in the y direction is zero. Instead of specifying thermal conditions on the ends, we use an equivalent energy flux condition[24]:

$$C = -\int_{-1/2}^{1/2} \frac{d\Psi}{dx} \theta \Big|_y dx \tag{19}$$

Using the approximations (17) and (18), the governing equations (11), (12) can be reduced to ordinary differential equations:

$$\frac{d^4\Psi}{dx^4} = Ra\left[\frac{d\theta}{dx}\sin\Phi + C\cos\Phi\right] \tag{20}$$

$$\frac{d^2\theta}{dx^2} = -C\frac{d\Psi}{dx} \tag{21}$$

which are now independent of Pr.

Solutions to (20) and (21) satisfying boundary conditions (6)–(9) are:

$$v = B(\cos ax \sinh ax + \gamma \sin ax \cosh ax) \tag{22}$$

$$\theta = \frac{CB}{2a^2}(\sin ax \cosh ax - \gamma \cos ax \sinh ax) - Cx \cot \Phi \tag{23}$$

where

$$a = (RaC \sin \Phi)^{0.25}/\sqrt{2}, \qquad b = a/2 \tag{24}$$

$$\gamma = \frac{\sin b \sinh b - \cos b \cosh b - (N \cos b \sinh b)/a}{\sin b \sinh b + \cos b \cosh b + (N \sin b \cosh b)/a} \tag{25}$$

$$B = \frac{2a(1 + C \cot \Phi)}{C[(1 - \gamma)\cos b \cosh b + (1 + \gamma)\sin b \sinh b]} \tag{26}$$

To obtain an equation for the constant C, condition (19) together with (22) to (26) can be used to give:

$$\frac{B^2}{16a^3}[4a\gamma + (1 - 2\gamma - \gamma^2)\sin a \cosh a - (1 + 2\gamma - \gamma^2)\cos a \sinh a] +$$

$$\frac{B}{a^2}\cot \Phi[\sin b \cosh b - \gamma \sinh b \cos b - b(1 + \gamma)\sinh b \sin b - b(1 - \gamma)\cosh b \cos b] - 1 = 0 \tag{27}$$

Transcendental equations (24)–(27) have to be simultaneously solved for the unknowns C, B, a and γ. This is done numerically by using a Newton–Raphson scheme. Real values of the constants can always be found for any Ra and Φ. The velocity and temperature fields are then known from (22) and (23).

Substituting (23) into (15) yields the Nusselt number as:

$$Nu = \frac{1}{\dfrac{2(1 + C \cot \Phi)}{a}\dfrac{\left[1 + \dfrac{N(\cosh^2 b - \cos^2 b)/a}{\sin b \cos b + \sinh b \cosh b}\right]}{\left[N/a + \dfrac{2(\cos^2 b + \sinh^2 b)}{\sin b \cos b + \sinh b \cosh b}\right]} - C \cot \Phi} \tag{28}$$

Vertical layer

We consider here the case of a vertical layer for which $\Phi = 90°$. Of particular interest is the boundary layer regime for which $Ra \to \infty$. An asymptotic analysis of (22) to (28) shows that the flow and temperature fields and the Nusselt number are given respectively by:

$$v = \frac{2ae^{a\bar{x}}}{C\left(2 + \dfrac{N}{a}\right)}\left[\cos a\bar{x} - \left(1 + \frac{N}{a}\right)\sin a\bar{x}\right] \tag{29}$$

$$\theta = \frac{e^{a\bar{x}}}{a\left(2 + \dfrac{N}{a}\right)}\left[\left(1 + \frac{N}{a}\right)\cos a\bar{x} + \sin a\bar{x}\right] \tag{30}$$

$$Nu = \frac{a\left(2 + \frac{N}{a}\right)}{2\left(1 + \frac{N}{a}\right)} \tag{31}$$

with $\bar{x} = x - 1/2$.

In the above equations, the value of the temperature gradient C is given by:

$$C = \sqrt{\frac{1}{2a}\left[1 - \frac{2a^2}{(2a+N)^2}\right]} \tag{32}$$

while the parameter a can be evaluated from:

$$\frac{a^9(2a+N)^2}{2a^2 + 4aN + N^2} = \frac{(Ra)^2}{32} \tag{33}$$

The convective heat transfer in a vertical fluid layer bounded by porous lining and heated from the side by a constant heat flux has been studied in the past by Murthy and Rudraiah[11]. A closed form solution was obtained by these authors from an Oseen-linearized analysis of the boundary layer regime. Their results, when written in the present notation, are equivalent to (29) to (33).

The heat transfer across a vertical fluid layer bounded by solid walls is obtained by taking the limit of (31) and (33), when $N \to \infty$, as:

$$Nu = \frac{a}{2} = 0.34(Ra)^{2/9} \tag{34}$$

This is a result predicted in the past by Kimura and Bejan[25].

As the value of $N \to 0$ it is found from (31) and (33) that the Nusselt number becomes:

$$Nu = a = 0.63(Ra)^{2/9} \tag{35}$$

Equations (34) and (35) indicate that the Nusselt number is increased approximately by a factor of two as the value of N is decreased from infinity to zero. However, the case with $N = 0$ corresponds to a fluid layer with free vertical surfaces and thus is not realistic.

Horizontal layer

The case of a horizontal fluid layer heated from below will now be considered. In this situation the governing equations are given by substituting $\Phi = 0$ into (20) and (21). The thermal boundary conditions, (6) and (7) still apply and the following hydrodynamic boundary conditions on the upper and lower horizontal boundary surfaces will be considered. The fact that the flow remains unicellular, in the case of a horizontal fluid layer heated from below by a constant heat flux, has been demonstrated by Vasseur *et al.*[21]. However, such a parallel flow is expected to become unstable as Ra is made large, giving rise to a multicellular flow similar to the classical Bénard cells observed in a fluid layer heated isothermally from below.

Both boundaries bounded by a porous lining

For this situation we consider that the fluid layer is bounded on each horizontal side by a porous layer made up of a different material. Then, the hydrodynamic boundary conditions,

(9); become:

$$\left.\begin{aligned} x = 1/2 \qquad & \frac{dv}{dx} = -N_1 v \\ x = -1/2 \qquad & \frac{dv}{dx} = -N_2 v \end{aligned}\right\} \tag{36}$$

Applying the same procedure as before, it is found that the velocity and temperature fields are given by:

$$v = \frac{RaC}{48}[-8x^3 + C_1(12x^2 - 1) + 2C_2] \tag{37}$$

$$\theta = \frac{RaC^2}{48}\left[-\frac{x}{40}(-16x^4 + 5) + \frac{C_1 x^2}{2}(2x^2 - 1) + \frac{C_2 x}{12}(4x^2 - 3)\right] + x \tag{38}$$

with

$$C_1 = (N_2 - N_1)/F$$

$$C_2 = [36 + 6(N_1 + N_2) + N_1 N_2]/F$$

$$F = 12 + 4(N_1 + N_2) + N_1 N_2$$

The constant C is now given by:

$$C = \pm\sqrt{\frac{1008(5C_2 - 3)[Ra - Ra_C]}{Ra^2[12C_1^2 + 21C_2^2 - 2C_2 + 7]}} \tag{39}$$

where Ra_C, the critical Rayleigh number for the onset of convection, is:

$$Ra_C = \frac{1440}{(5C_2 - 3)} \tag{40}$$

From (39) it is seen that for $Ra < Ra_C$, $C = 0$ is the only real solution (it stays stable). For $Ra > Ra_C$ a unicellular convection motion, rotating either clockwise ($C < 0$) or counter clockwise ($C > 0$), bifurcates from the rest state. The present analysis can predict the critical Rayleigh number Ra_C since, as demonstrated by Sparrow *et al.*[29], this happens at zero-wave number (parallel flow) for a layer heated from bottom by a constant heat flux.

Substituting (38) into (15) yields the Nusselt number as:

$$Nu = \frac{1440}{\dfrac{1008(5C_2 - 3)^2[Ra - Ra_C]}{Ra[12C_1^2 + 3C_2(7C_2 - 8) + 7]} + 1440} \tag{41}$$

The following cases are of practical interest:

Both horizontal boundaries are solid ($N_1, N_2 \to \infty$). For this case, $C_1 = 0$ and $C_2 = 1$. From the above equations it is readily shown that:

$$Ra_C = 720 \tag{42}$$

which has already been predicted by Sparrow *et al.*[29].

Also, from (40), the Nusselt number is given by:

$$= \frac{10}{3 + \dfrac{5040}{Ra}} \tag{43}$$

which yields $Nu = 10/3$ when $Ra \to \infty$ in agreement with the previous results given by Vasseur *et al.*[21].

Both horizontal boundaries are free ($N_1 = N_2 = 0$). For this situation, $C_1 = 0$ and $C_2 = 3$ such that, according to (39), the critical Rayleigh number is:

$$Ra_C = 120 \tag{44}$$

which has already been predicted in the past by Sparrow *et al.*[29].

The Nusselt number, (40), is reduced to:

$$Nu = \frac{155}{29 + \dfrac{15120}{Ra}} \tag{45}$$

which gives $Nu = 5.34$ when $Ra \to \infty$.

Lower surface rigid, upper free ($N_1 \to \infty$, $N_2 = 0$). For this situation, $C_1 = 1/4$ and $C_2 = 3/2$ and the critical Rayleigh number is:

$$Ra_C = 320 \tag{46}$$

which is in agreement with the results of Sparrow *et al.*[29]. The Nusselt number is:

$$Nu = \frac{760}{193 + \dfrac{181440}{Ra}} \tag{47}$$

Upper surface free and lower surface bounded by a porous lining

Here it is assumed that the upper boundary of the liquid layer is open to ambient air. Thermocapillary forces acting at the free surface are taken into account. The lower surface is bounded by a porous lining. The resulting boundary conditions are:

$$x = 1/2 \qquad \frac{dv}{dx} = -Nv \tag{48}$$

$$x = -1/2 \qquad \frac{dv}{dx} = Ma\frac{\partial T}{\partial y} \tag{49}$$

where Ma is the Marangoni number, defined as:

$$Ma = \frac{Sq'L'^2}{\alpha\mu k} \tag{50}$$

in which S is the surface tension gradient with respect to the temperature, i.e., $S = -\partial\sigma/\partial T'$.

For this situation it may be shown that the temperature and velocity fields are given respectively by:

$$v = \frac{RaC}{192}\frac{1}{(3+N)}[24x(-4x^2+3) + N(-32x^3 - 12x^2 + 12x + 1)] + \frac{MaC}{6}\frac{1}{(3+N)}[2(-12x^2 + 12x + 1) + N(-12x^2 + 4x + 1)] \tag{51}$$

$$\theta = \frac{RaC^2}{1920}\frac{1}{(3+N)}[3x(-16x^4+40x^2-25)+Nx(-16x^4-10x^3+20x^2+5x-10)]+$$
$$\frac{MaC^2}{96}\frac{1}{(3+N)}[2x(-6x^3+12x^2+3x-9)+Nx(-6x^3+4x^2+3x-3)]+x \tag{52}$$

In the above equations the temperature gradient C is:

$$C = \pm(3+N)\sqrt{\frac{1451520\left[\frac{Ra(8+N)}{320(3+N)}+\frac{Ma(6+N)}{48(3+N)}-1\right]}{Den}} \tag{53}$$

where Den is given by:

$$Den = Ra^2(1116+285N+19N^2)+36RaMa(306+91N+7N^2)+864Ma^2(32+11N+N^2)$$

and the threshold value for the onset of Bénard–Marangoni convection is given by:

$$\frac{Ra_C}{320}\frac{(8+N)}{(3+N)}+\frac{Ma_C}{48}\frac{(6+N)}{(3+N)}=1 \tag{54}$$

Of particular interest is the case of a fluid layer bounded at the bottom by a solid wall for which $N \to \infty$. For this situation, (54) reduces to:

$$\frac{Ra_C}{320}+\frac{Ma_C}{48}=1 \tag{55}$$

The Nusselt number for the present situation is obtained as:

$$Nu = \frac{1}{1-\frac{C^2}{16(3+N)}\left[\frac{(8+N)}{20}Ra+\frac{(6+N)}{3}Ma\right]} \tag{56}$$

which agrees with the predictions of Nield[30]. Thus, under microgravitational condition ($Ra_C = 0$) the onset of convection in a surface tension driven fluid layer occurs at $Ma_C = 48$.

RESULTS AND DISCUSSION

Based on the governing equations of motion and energy, it follows that the parameters affecting the convective heat transfer in the present problem are Rayleigh and Prandtl numbers Ra and Pr, slip condition parameter N, aspect ratio of the cavity A and inclination angle Φ. It has been demonstrated numerically by Vasseur *et al.*[21] that, in the case of a cavity heated by a constant heat flux, the solution is independent of A provided that A is made larger than approximately 3. For this reason all the numerical results presented in this study were obtained for $A = 4$. Also, a Prandtl number of 0.71 was used in all the numerical calculations since the solution is almost independent of this parameter. The ranges of parameters considered in the present study are $1 \leqslant Ra \leqslant 10^7$, $0 \leqslant N \leqslant \infty$ and $0 \leqslant \Phi \leqslant 180°$. In the following section the effect of different parameters are discussed.

Typical numerical results are presented in *Figure 2* which shows the streamline and isotherm patterns obtained for $Ra = 10^6$, $\Phi = 90°$ and $N = \infty$, 50, 10 and 0, respectively. The corresponding vertical velocity and temperature profiles, at mid-height of the vertical cavity, are plotted in *Figure 3* and it is seen that the agreement between the analytical and the numerical

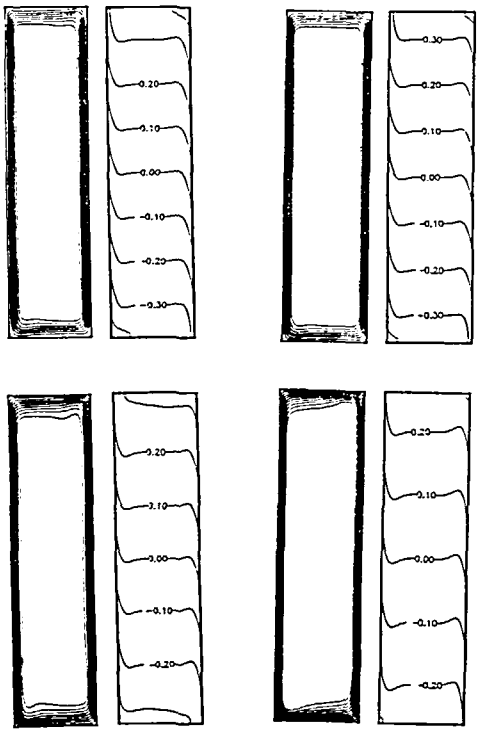

Figure 2 Numerical solutions for the flow and temperature field for $Ra = 10^6$, $A = 4$, $\Phi = 90°$; (a) $N = \infty$, $\Psi_{max} = 9.1954$, $T_{max} = 0.4874$, $T_{min} = -0.4874$; (b) $N = 50$, $\Psi_{max} = 9.4581$, $T_{max} = 0.4603$, $T_{min} = -0.4603$; (c) $N = 10$, $\Psi_{max} = 10.4792$, $T_{max} = 0.3975$, $T_{min} = -0.3975$; (d) $N = 0$, $\Psi_{max} = 12.1108$, $T_{max} = 0.3275$, $T_{min} = -0.3275$

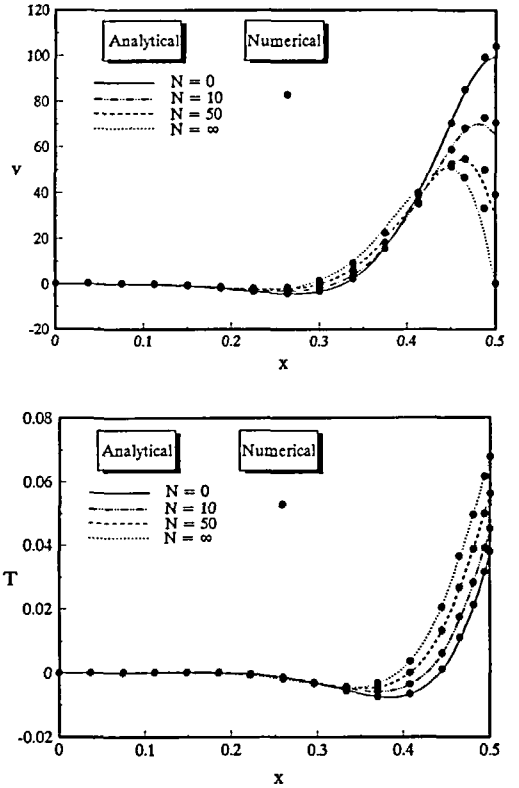

Figure 3 (a) The vertical velocity profile at mid-height of the cavity as a function of BJ number N for $Ra = 10^6$ and $\Phi = 90°$. (b) The temperature profile at mid-height of the cavity as a function of BJ number N for $Ra = 10^6$ and $\Phi = 90°$

results is excellent. In *Figure 2*, the increment between adjacent streamlines and isotherms are $\Delta\Psi = 1$ and $\Delta T = 0.1$ respectively. *Figure 2a* illustrates the results obtained when the fluid layer is bounded by rigid impermeable walls, i.e. for $N \to \infty$ and the fluid not allowed to slip on the boundaries. This situation has been discussed in the past by Kimura and Bejan[25] and Vasseur *et al.*[21]. The pattern of streamlines of *Figure 2a* shows that the core fluid is stagnant while a boundary layer of constant thickness develops near the vertical boundaries (see also *Figure 3a*). From the equal spacing of the isotherms, a linear thermal vertical stratification is deduced both in the core and vertical boundary layers. In fact, as demonstrated by Kimura and Bejan[25], the temperature between vertical walls is independent of altitude since the wall temperatures increase linearly at the same rate as the vertical temperature gradient in the core region. *Figures 2b–2d* illustrate typical results for various values of N. As the value of N decreases, the streamlines are observed to become more and more closely spaced near the porous boundaries. This is due to the fact that, due to BJ conditions prescribed at the porous–fluid interface, the fluid is now progressively allowed to slip on the bounding walls as illustrated in *Figure 3a*. Thus, as N decreases, the viscous forces near the boundaries become relatively less important and the fluid circulation within the cavity is enhanced as indicated by the values of Ψ_{max}.

The Nusselt number Nu for a vertical cavity ($\Phi = 90°$) is presented in *Figure 4* as a function of Ra for selected values of the parameter N. The analytical results are continuous line; numerical

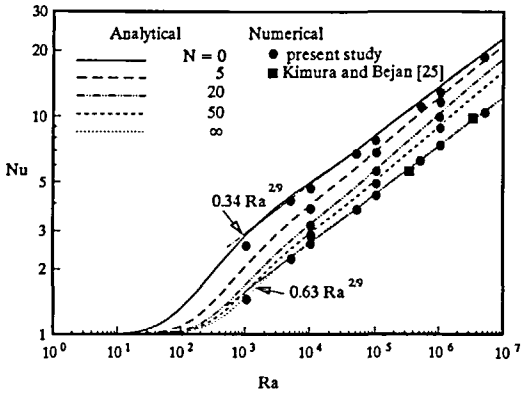

Figure 4 Effect of Rayleigh number *Ra* and BJ number *N* on the Nusselt number for a vertical cavity ($\Phi = 90°$)

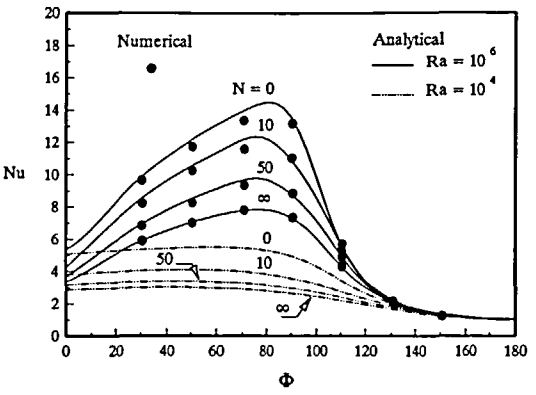

Figure 5 Effect of inclination angle Φ and BJ number *N* on Nusselt number *Nu* for $Ra = 10^4$ and 10^6

results shown as solid circles are seen to agree well. The numerical results of Kimura and Bejan[25] for the limiting case of $N \to \infty$, i.e. a fluid layer bounded by rigid walls, are also shown, with good agreement. The heat transfer results in the boundary layer regime, (34) and (35), for $N \to \infty$ and $N \to 0$ respectively, are also plotted on this graph for comparison. The boundary layer regime is seen to be reached at $Ra \geqslant 5 \times 10^3$ and this, independently of the value of N. It is clear from *Figure 4* that *Nu* decreases with increasing N. This is expected since, due to BJ conditions, the flow circulation is progressively inhibited due to the presence of increasing viscous forces near the bounding walls. As a result the difference of temperature ΔT between the thermally active walls increases (see *Figure 3b*), thus causing a lower Nusselt number.

Figure 5 presents the results for Nusselt number *Nu* as a function of inclination Φ for Rayleigh numbers *Ra* of 10^4 and 10^6 and various values of the slip condition parameter N. Also shown in the Figure are results of numerical calculations and an excellent agreement with the analytical solution is observed in the range of parameters considered. The inclination angle Φ is seen to have a dominant effect on the Nusselt number for given values of *Ra* and N. As the inclination angle Φ approaches 180°, the Nusselt number tends towards unity, indicating that the heat transfer is mainly due to conduction. This is expected since $\Phi = 180°$ corresponds to the case of a cavity heated from the top which causes no convection as the density gradient is stable. As the inclination angle Φ is decreased from 180° to 0° the Nusselt number starts to increase first, passes through a peak and then begins to decrease. The peak in the Nusselt number is a function of both *Ra* and N. A similar trend has been reported in the case of inclined cavities with two opposite isothermal rigid surfaces ($N \to \infty$) maintained at different temperatures (see for instance References 26–27).

The critical Rayleigh number Ra_C marking the onset of instability in a horizontal fluid layer heated from below is plotted in *Figure 6* as a function of N_1 and N_2, the slip condition parameters at the lower and upper boundaries respectively. The solid curves are the results of (40). As mentioned earlier, the critical Rayleigh number $Ra_C = 320$, for a fluid layer with a free surface and a solid boundary ($N_1 \to 0$ and $N_2 \to \infty$, or $N_1 \to \infty$ and $N_2 \to 0$) has been predicted in the past by Hurle *et al.*[28] using a linear stability analysis. On the other hand, the values $Ra_C = 720$ and $Ra_C = 120$, for the case of a fluid layer bounded by two solid boundaries ($N_1, N_2 \to \infty$) and with both boundaries free ($N_1, N_2 \to 0$), have been obtained by Sparrow *et al.*[29]. All these results are presented as broken lines in *Figure 6*. For intermediate values of N_1 and N_2 a smooth transition of the curves between these limits is observed.

The variation of *Nu* with *Ra* and N is illustrated in *Figure 7* for the case of a horizontal fluid layer heated from below and bounded by porous boundaries made up of the same material

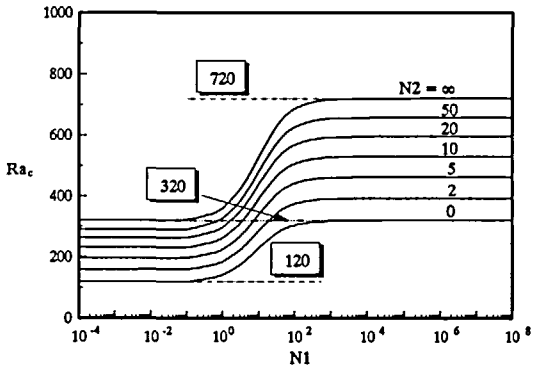

Figure 6 Critical Rayleigh number Ra_C as a function of BJ numbers N_1 and N_2 for bottom heating

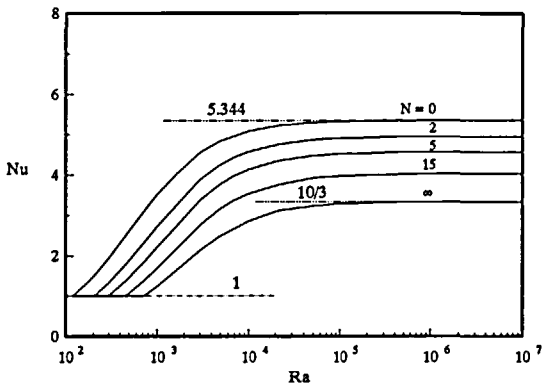

Figure 7 Nusselt number Nu as a function of Rayleigh number Ra for selected values of BJ number N

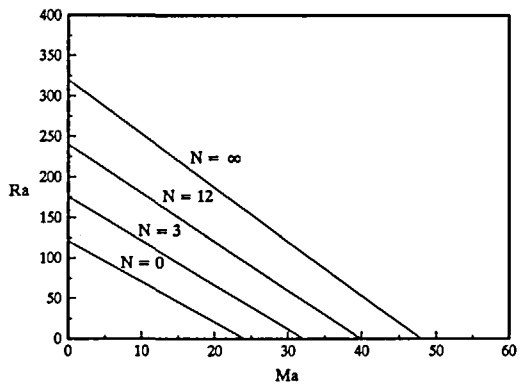

Figure 8 Stability curves for a horizontal fluid layer with upper free surface and bottom porous lining

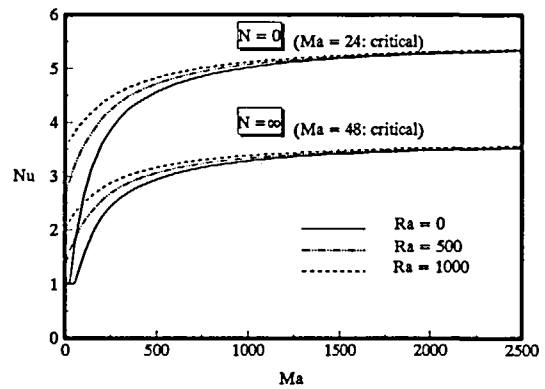

Figure 9 Nusselt number Nu as a function of Ma for selected values of Ra and N for a horizontal fluid layer with upper free surface and bottom porous lining

($N_1 = N_2 = N$). For a given N, there is a critical Rayleigh number Ra_C, (40), below which convection is not possible (pure conduction state). Thus for each of N considered in *Figure 7*, the Nusselt number approaches the pure conduction solution ($Nu = 1$), as Ra tends towards the value of the corresponding critical Rayleigh number. When Ra is higher than Ra_C, the Nusselt number is seen to increase as usual with Ra. However, it is clear from *Figure 7* that at higher Ra, Nu tends asymptotically towards a constant value which depends upon N.

Figure 8 shows the marginal stability curves, (54), for the case of a fluid layer heated from below when its upper boundary is a free surface. In this case, the Marangoni force plays an important role in the initiation of the fluid motion. The curves in *Figure 8* are plotted for selected values of N, the slip condition parameter at the interface between the bottom of the fluid layer and the porous lining. When $N \to \infty$, the bottom wall is rigid and impermeable and the results predicted by Garcia-Ybarra *et al.*[31] are recovered. Thus, when the Marangoni effect is negligibly small, the critical Rayleigh number for the onset of fluid motion with upper free surface and a lower rigid boundary is $Ra_C = 320$, which is the same as that obtained by Sparrow *et al.*[29]. Under microgravitational condition, the motion at the onset corresponds to a threshold value for the Marangoni number of $Ma_C = 48$. From an inspection of *Figure 8*, it is seen that the

critical Rayleigh and Marangoni numbers decrease monotonically with decreasing parameter N. Thus the most stable situation corresponds to a rigid impermeable lower wall ($N \to \infty$) while the most unstable situation corresponds to a free lower boundary ($N \to 0$). In the latter case $Ra_c = 120$ when $Ma = 0$, as predicted by Hurle *et al.*[28], while $Ma_c = 24$ when $Ra \to 0$. The fact that the most stable situation corresponds to $N \to \infty$ agrees with an intuitive feeling that a fluid layer bounded by a rigid surface should be more stable than a fluid layer with a free surface.

Figure 9 shows the dependence of the Nusselt number Nu on Ma and Ra for a horizontal fluid layer heated from below with an upper free surface. The results are presented for $N = \infty$ (rigid impermeable lower surface) and $N = 0$ (free lower boundary). For a given Ra there is a critical Marangoni number Ma_c, (54), below which the fluid layer is stable. *Figure 9* indicates that, in general, the Nusselt number increases with either Ma or Ra. This is expected since these two parameters promote convective circulation within the fluid layer, which reduces the temperature difference between the two horizontal boundaries, thus causing a higher Nusselt number. For the same reason Nusselt numbers obtained for $N = 0$ are higher than those for $N = \infty$ since the convective flow is promoted as the value of the parameter N is reduced, i.e. as the fluid is progressively allowed to slip over the porous lining.

CONCLUSIONS

The problem of natural convection heat transfer in a two-dimensional inclined fluid layer bounded by porous layers with uniform heat flux from two opposite walls while the others are insulated has been studied both numerically and analytically. Solutions are obtained using the Beavers–Joseph condition as the interface condition on velocity between the fluid and porous layers. The analytical solution, based on a parallel flow approximation, reveals in closed form, the roles played by the BJ-slip condition at the interface, the Rayleigh number Ra and the inclination angle Φ. The main conclusions of the present analysis are:

(1) For a given Rayleigh number Ra and cavity inclination angle Φ the effect of slip parameter N is to increase both the convective flow and the Nusselt number. The cavity inclination, for given values of Ra and N, has a large effect on the heat transfer rate. As the inclination angle increases from 0° to 180° the heat transfer starts to increase first, passes through a peak and then begins to decrease. The peak in the Nusselt number is a function of both Ra and N.

(2) In the case of a vertical cavity heated from the side ($\Phi = 90°$) the solution predicted by the present study for boundary-layer regime ($Ra \to \infty$) is in agreement with Murthy and Rudraiah's result[11] obtained by solving the boundary layer equations by a linearization technique. However, the present analysis extends their solution to the low Rayleigh number regime.

(3) The case of a horizontal fluid layer ($\Phi = 0$), heated from the bottom, has been considered for various hydrodynamic boundary conditions. The prediction of the critical Rayleigh number is correctly obtained from the present parallel-flow analysis because the convection that occurs when a constant heat flux is applied to a horizontal fluid layer, is at zero wave number. It is shown that the results of a fluid layer with solid–solid ($N \to \infty$) and free–free ($N \to 0$) boundaries emerge from the present solution as special cases. The effect of the Marangoni number on both critical Rayleigh number and heat transfer is also considered.

The main features of the approximate theoretical solutions have been tested by a numerical solution of the full governing equations in the range of $1 \leqslant Ra \leqslant 10^7$, $0 \leqslant N \leqslant \infty$ and $0 \leqslant \Phi \leqslant 180°$.

ACKNOWLEDGEMENTS

This work was supported in part by the Natural Sciences and Engineering Research Council of Canada and jointly by the FCAR Government of Quebec.

REFERENCES

1 Bejan, A. *Convection Heat Transfer*, John Wiley, New York (1984)
2 Somerton, C. W. and Catton, I. On the thermal instability of superposed porous and fluid layers, *J. Heat Transfer*, **104**, 160–165 (1982)
3 Arquis, E. and Caltagirone, J. P. Interacting convection between fluid and open porous layers, *ASME Winter A. Meet., Boston*, **87** (WA/HT-24) (1987)
4 Nishimura, T., Takumi, T., Shiraishi, M., Kawamura, Y. and Ozoe, H. Numerical analysis of natural convection in a rectangular horizontally divided into fluid and porous region, *Int. J. Heat Mass Transfer*, **26**, 889–898 (1986)
5 Vasseur, P., Wang, C. H. and Sen, M. Thermal instability and natural convection in a fluid layer over a porous substrate, *Waerme-Stoffuebertra.*, **24**, 337–347 (1989)
6 Beavers, G. S. and Joseph, D. D. Boundary conditions at a naturally permeable wall, *J. Fluid Mech.*, **30**, 197–207 (1967)
7 Nield, D. A. Onset of convection in a fluid layer overlying a layer of porous medium, *J. Fluid Mech.*, **81**, 513–522 (1977)
8 Nield, D. A. Boundary correction for the Rayleigh–Darcy problem: limitations of the Brinkman equation, *J. Fluid Mech.*, **128**, 37–46 (1983)
9 Pillatsis, G., Taslin, M. E. and Narusawa, U. Thermal instability of a fluid-saturated porous medium bounded by thin fluid layers, *J. Heat Transfer*, **109**, 677–682 (1987)
10 Chen, F., Chen, C. F. and Pearlstein, A. J. Convective instability in superposed fluid and anisotropic porous layers, *Phys. Fluids*, **4**, 556–565 (1991)
11 Murthy, J. K. S. and Rudraiah, N. Closed form solution for natural convection in a vertical slot bounded by porous layer, *Fourth Asian Congr. Fluid Mech.*, **1**, H17–H20 (1989)
12 Taylor, G. I. A model for the boundary condition of a porous material, Part I, *J. Fluid Mech.*, **49**, 319–326 (1971)
13 Richardson, S. A model for the boundary condition of a porous material, Part II, *J. Fluid Mech.*, **49**, 327–336 (1971)
14 Beavers, G. S., Sparrow, E. M. and Magnuson, R. A. Experiments on coupled parallel flows in a channel and a bounding porous medium, *J. Basic Eng.*, **92**, 843–848 (1970)
15 Beavers, G. S., Sparrow, E. M. and Masha, B. A. Boundary conditions at a porous surface which bounds a fluid flow, *AIChE J.*, **1**, 596–597 (1974)
16 Patankar, S. V. *Numerical Heat Transfer and Fluid Flow*, Hemisphere, New York (1980)
17 De Vahl Davis, G. and Jones, I. P. Natural convection as a square cavity: a comparison exercise, *Int. J. Num. Meth. Fluids*, **3**, 227–248 (1983)
18 Cormack, D. E., Leal, L. G. and Imberger, J. Natural convection in a shallow cavity with differentially heated end walls, Part 1: Asymptotic theory, *J. Fluid Mech.*, **65**, 209–229 (1974)
19 Bejan, A. and Tien, C. L. Laminar natural convection heat transfer in a horizontal cavity with different end temperatures, *J. Heat Transfer*, **100**, 641–647 (1978)
20 Vasseur, P., Wang, C. H. and Sen, M. The Brinkman model for natural convection in a shallow porous cavity with uniform heat flux, *Num. Heat Transfer*, **15**, 221–242 (1989)
21 Vasseur, P., Robillard, L. and Sen, M. Unicellular convective motion in an inclined fluid layer with uniform heat flux, *Bifurcation Phenomena in Thermal Processes and Convection* (ASME HTD), **94**, 23–29 (1987)
22 Sen, M., Vasseur, P. and Robillard, L. Multiple steady states for unicellular natural convection in an inclined porous layer, *Int. J. Heat Mass Transfer*, **30**, 2097–2113 (1987)
23 Sen, M., Vasseur, P. and Robillard, L. Parallel flow convection in a tilted two-dimensional porous layer heated from all sides, *Phys. Fluids*, **31**, 3480–3487 (1988)
24 Bejan, A. The boundary layer regime in a porous layer with uniform heat flux from the side, *Int. J. Heat Mass Transfer*, **26**, 1339–1346 (1983)
25 Kimura, S. and Bejan, A. The boundary layer natural convection regime in a rectangular cavity with uniform heat flux from the side, *J. Heat Transfer*, **106**, 98–103 (1984)
26 Inaba, H. and Kanayama, K. Natural convection heat transfer in an inclined rectangular cavity, *Bull. JSME*, **27**, 1702–1708 (1984)
27 Chen, C. J. and Talaie, V. Finite analytic numerical convection in two-dimensional inclined rectangular enclosures, *National Heat Transfer Conf.*, **85-HT-10** (1985)
28 Hurle, D. T. J., Jakeman, E. and Pike, E. R. On the solution of the Bénard problem with boundaries of finite conductivity, *Proc. R. Soc. Lond.*, **A296**, 469–475 (1967)
29 Sparrow, E. M., Goldstein, R. J. and Jonsson, V. K. Thermal instability in a horizontal fluid layer: effect of boundary conditions and non-linear temperature profile, *J. Fluid Mech.*, **18**, 513–528 (1964)
30 Nield, D. A. Surface tension and buoyancy effects in cellular convection, *J. Fluid Mech.*, **51**, 341–352 (1964)
31 Garcia-Ybarra, P. L., Castillo, J. L. and Velarde, M. G. Bénard–Marangoni convection with deformable interface and poorly conducting boundaries, *Phys. Fluids*, **30**, 2655–2661 (1987)